CHAPTER ONE HUNDRED NINETY SEVEN

DYNAMIC ANALYSIS OF PILE STRUCTURES
TO PERIODIC WAVES

Hajime Ishida
Associate Professor, Department of Civil Engineering,
Kanazawa University, Kanazawa, Japan

and

Yoshinori Konda
Staff, Aichi Prefectural Government, Nagoya, Japan

ABSTRACT

This paper has dealt with the dynamic response of offshore
structures to the ocean waves. In order to establish the calculation
scheme for offshore structures, the methods of transfer matrices and of
structural-property matrices have been introduced and applied to the
analysis of dynamic response of pile structures. The validity of these
calculation methods have been verified by the experiments in the
laboratory.

INTRODUCTION

The need for drilling oil from the sea bed has induced the progress
of ocean structures until now, and much more structures should be
constructed to extract the new sources and energies from the oceans in
the future. Then, more precise design of structures should be demanded
with considering the dynamic behaviours from the viewpoint of
reliability and economical efficiency.

The purpose of this paper is to advance the calculation scheme of
dynamic analysis of offshore structures and to clarify the
characteristics of the dynamic response to waves. The structural forms
treated in this paper are as follows: (1) a vertical small diameter
pile, (2) a platform supported by four small diameter piles and (3) a
vertical large diameter pile. These three structures are analysed with
modeling as a multi-degrees-of freedom system by using the methods of
transfer matrices and of structural-property matrices.

The method of transfer matrices is suitable for the analysis of
harmonic vibrations, and this method has already been applied to the
vibrational analysis of offshore structures by Gaither and Billington[1]
However, only the monochromatic concentrating forces were used as the

external forces and no calculations have been performed by using the
wave forces in their study. Then, in this paper, the authors advance
their study and indicate the calculation method for the ocean waves. In
the case of a small diameter pile, not only the small amplitude wave
theory but also the Stokes wave theory are applied to the Morison's
formula to explain the resonant characteristics. In the case of a large
diameter pile, MacCamy-Fuchs' diffraction theory[2] is used as the equation
of wave force in stead of Morison's formula.

     The method of structural-property matrices[3] is convenient for
calculating the transient response with including the initial conditions
or the random vibrations induced by irregular waves. In this paper, this
calculation method and the results of some model calculations are shown
mainly in the case of periodic waves.

     In order to discuss the validity of these calculation methods and
to find the characteristics of real vibrations, the laboratory
experiments are conducted in the wave tanks by using the model
structures mentioned above.

METHOD OF TRANSFER MATRICES

### EVALUATION OF TRANSFER MATRICES[1]

     The coordinate system is shown in Fig.1. The share force in the
direction of the z-axis and the corresponding displacement are denoted
by V_z and w respectively. The bending moment around the y-axis and the
corresponding slope are denoted by M_y and ψ respectively. Henceforth, V_z,
M_y, w and ψ are used as the complex amplitudes. The amplitudes are
generated by eliminating from their real quantities the time part
oscillating with an angular frequency Ω, $exp(j\Omega t)$, in which t is the
time and $j=\sqrt{-1}$.

     The vertical column vector constructed by their real and imaginary
parts is called the state vector and is denoted by $\{z\}$ as follows:

$$\{z\}=\{-w, \psi, M_y, V_z \mid -w, \psi, M_y, V_z \mid 1\}^T \cdots (1)$$
$$\underbrace{\qquad\qquad}_{\text{Real}} \underbrace{\qquad\qquad}_{\text{Imaginary}} \underbrace{\quad}_{\text{Unit}}$$

To apply the method of transfer
matrices, the continuous member is
idealized as a discrete series of
masses and beams as shown in Fig.2.
The external forces are considered
to act upon the masses.

     Using the compatibility and
equilibrium conditions at the beam
i, the relationship between the
state vector of the upper side of
the mass i-1 denoted by $\{z\}^U_{i-1}$, and
that of lowere side of the mass i
denoted by $\{z\}^L_i$, can be described by
the matrix equation
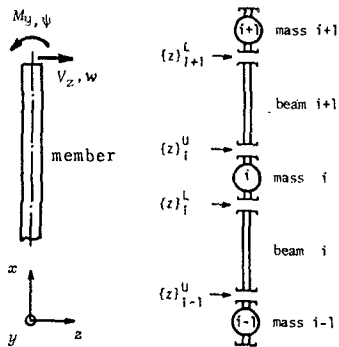
Fig.1 Coordinate   Fig.2 Mass-beam
      system[4].   system[4].

$${z}_i^L = [F]_i {z}_{i-1}^U , \qquad \cdots\cdots\cdots\cdots\cdots\cdots\cdots\cdots\cdots\cdots(2)$$

in which $[F]_i$ is called the field transfer matrix and given by

$$[F]_i = \begin{bmatrix} 1 & L & \dfrac{L^2}{2EI(1+\epsilon^2)} & \dfrac{L^3}{6EI(1+\epsilon^2)} & \vdots & 0 & 0 & \dfrac{\epsilon L^2}{2EI(1+\epsilon^2)} & \dfrac{\epsilon L^3}{6EI(1+\epsilon^2)} & \vdots & 0 \\ 0 & 1 & \dfrac{L}{EI(1+\epsilon^2)} & \dfrac{L^2}{2EI(1+\epsilon^2)} & \vdots & 0 & 0 & \dfrac{\epsilon L}{EI(1+\epsilon^2)} & \dfrac{\epsilon L^2}{2EI(1+\epsilon^2)} & \vdots & 0 \\ 0 & 0 & 1 & L & \vdots & 0 & 0 & 0 & 0 & \vdots & 0 \\ 0 & 0 & 0 & 1 & \vdots & 0 & 0 & 0 & 0 & \vdots & 0 \\ \cdots & & & & & & & & & & \\ 0 & 0 & \dfrac{-\epsilon L^2}{2EI(1+\epsilon^2)} & \dfrac{-\epsilon L^3}{6EI(1+\epsilon^2)} & \vdots & 1 & L & \dfrac{L^2}{2EI(1+\epsilon^2)} & \dfrac{L^3}{6EI(1+\epsilon^2)} & \vdots & 0 \\ 0 & 0 & \dfrac{-\epsilon L}{EI(1+\epsilon)^2} & \dfrac{-\epsilon L^2}{2EI(1+\epsilon^2)} & \vdots & 0 & 1 & \dfrac{L}{EI(1+\epsilon^2)} & \dfrac{L^2}{2EI(1+\epsilon^2)} & \vdots & 0 \\ 0 & 0 & 0 & 0 & \vdots & 0 & 0 & 1 & L & \vdots & 0 \\ 0 & 0 & 0 & 0 & \vdots & 0 & 0 & 0 & 1 & \vdots & 0 \\ \cdots & & & & & & & & & & \\ 0 & 0 & 0 & 0 & \vdots & 0 & 0 & 0 & 0 & \vdots & 1 \end{bmatrix}_i \qquad \cdots\cdots\cdots(3)$$

In Eq.(3), E is the elastic modulus, A is the cross-sectional area, I is the second moment of inertia about the y-axis, L is the beam length between the two masses, and ϵ is a constant number driven by considering the structural damping to the beam. The range of values is commonly indicated as $\epsilon = 0 \sim 0.015$.

By applying the same conditions to the mass i, the relationship between the state vectors ${z}_i^U$ and ${z}_i^L$ is obtained as follows:

$${z}_i^U = [P]_i {z}_i^L , \qquad \cdots\cdots\cdots\cdots\cdots\cdots\cdots\cdots\cdots(4)$$

in which $[P]_i$ is the point transfer matrix and given by

$$[P]_i = \begin{bmatrix} 1 & 0 & 0 & 0 & 0 & \vdots & 0 & 0 & 0 & 0 & \vdots & 0 \\ 0 & 1 & 0 & 0 & 0 & \vdots & 0 & 0 & 0 & 0 & \vdots & 0 \\ 0 & I_y\Omega^2 & 1 & 0 & 0 & \vdots & 0 & c_\psi\Omega & 0 & 0 & \vdots & -f_\psi \\ m\Omega^2 & 0 & 0 & 1 & 0 & \vdots & c_z\Omega & 0 & 0 & 0 & \vdots & -f_z \\ \cdots & & & & & & & & & & & \\ 0 & 0 & 0 & 0 & 0 & \vdots & 1 & 0 & 0 & 0 & \vdots & 0 \\ 0 & 0 & 0 & 0 & 0 & \vdots & 0 & 1 & 0 & 0 & \vdots & 0 \\ 0 & -c_\psi\Omega & 0 & 0 & 0 & \vdots & 0 & I_y\Omega^2 & 1 & 0 & \vdots & 0 \\ -c_z\Omega & 0 & 0 & 0 & 0 & \vdots & m\Omega^2 & 0 & 0 & 1 & \vdots & 0 \\ \cdots & & & & & & & & & & & \\ 0 & 0 & 0 & 0 & 0 & \vdots & 0 & 0 & 0 & 0 & \vdots & 1 \end{bmatrix}_i \qquad \cdots\cdots(5)$$

In Eq.(5), m is the mass, I_y is the mass moment of inertia about the y-axis, and c_z and c_ψ are the coefficients of viscous damping in the direction of the z-axis and around the y-axis respectively. f_z and f_ψ are amplitudes of the external forces in the direction of the z-axis and the external moment around the y-axis respectively.

Fig.3 shows the pile idealized as the mass-beam system. Transferring the state
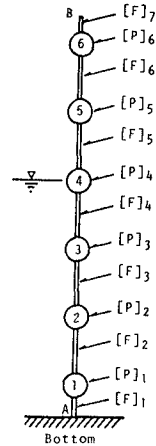
Fig.3 Idealized pile as mass-beam system[4].

vector $\{z\}$ from the fixed base at A to the free end at B by using Eqs. (2) and (4), the following equation which gives the relationship between the state vector at the location A denoted by $\{z\}_A$ and that of the location B denoted by $\{z\}_B$ is obtained:

$$\{z\}_B = [F]_7[P]_6[F]_6 \cdots [P]_1[F]_1\{z\}_A = [U]_{BA}\{z\}_A . \quad \cdots\cdots\cdots (6)$$

The boundary conditions for this case are given as follows:

$$
\begin{aligned}
&\text{for the location } A : w =0, \ \psi =0, \\
&\text{for the location } B : V_z=0, \ M_y=0.
\end{aligned} \quad \cdots\cdots\cdots\cdots\cdots (7)
$$

Substituting Eq.(7) to Eq.(6), M_y and V_z at the location A, and w and ψ at the location B can be obtained, that is $\{z\}_A$ and $\{z\}_B$ can be determined so as to satisfy the boundary conditions. The state vector of each location, therefore, can be calculated by using Eqs.(2),(4) and the state vector $\{z\}_A$.

EXTERNAL FORCE TERMS DUE TO WAVES

In the following, the coordinate system is taken as shown in Fig.4. ξ denotes the displacement of pile in the direction of the x-axis. u and $\dot{u}$ denote respectively the water particle velocity and its acceleration in the direction of the x-axis.

Applying Morison's formula and using the relative velocities to express the wave forces on the pile in the direction of the x-axis, the equation about the transverse vibration of pile is expressed as follows:

$$\rho A\xi_{tt} + c_1\xi_t + EI\xi_{zzzz} = \frac{1}{2}C_D\rho_w D(u - \xi_t) \mid u - \xi_t \mid$$

$$+ (C_M - 1) \rho_w A (\dot{u} - \xi_{tt}) + \rho_w A\dot{u} \quad \cdots\cdots (8)$$
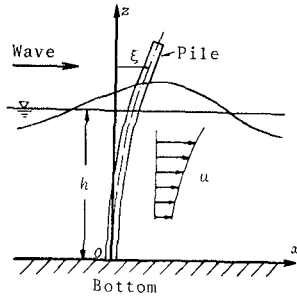
Fig.4 Coordinate system of wave field.

in which, ρ and ρ_w are the densities of pile and water respectively, c_1 is the damping coefficient, D is the diameter of pile, and C_D and C_M are the drag and inertia coefficients respectively. The lower indices of ξ, t and z, indicate the differentiation ξ with respect to t and z respectively.

Eq.(8) is nonlinear with respect to ξ, however, if the assumption that $u \gg \xi$ is made, the Eq.(8) becomes linear as follows:

$$(\rho A + K\rho_w A) \xi_{tt} + (c_1 + 2C_D' \mid u \mid) \xi_t + EI\xi_{zzzz} = C_D' u \mid u \mid + C_M'\dot{u} , \quad \cdots\cdots\cdots\cdots (9)$$

in which, $C_D' = C_D\rho_w D/2$, $C_M' = C_M\rho_w A$, $K = C_M - 1$, and K is called the added mass coefficient.

By using the small amplitude wave theory, the water level variation η, the water particle velocity u and its acceleration $\dot{u}$ at the location $x=0$ are described as follows:

$$\eta = a \cos \sigma t , \quad \cdots\cdots\cdots\cdots\cdots\cdots\cdots (10)$$

$$u = a\sigma (\cosh kz / \sinh kh) \cos \sigma t , \quad \cdots\cdots\cdots\cdots (11)$$

$$\dot{u} = -a\sigma^2 (\cosh kz / \sinh kh) \sin \sigma t . \quad \cdots\cdots\cdots\cdots (12)$$

Substituting Eqs.(11) and (12) into Eq.(9), and integrating Eq.(9) along the divided length $\Delta z_i = z_i - z_{i-1}$ shown in Fig.5, m_i and c_{z_i} included in $[P]_i$ of Eq.(5) can be obtained as follows:

$$m_i = (\rho A + K \rho_w A) \Delta z_i , \quad \cdots\cdots\cdots\cdots\cdots\cdots (13)$$

$$c_{z_i} = c_1 \Delta z_i + 2 C_D' a\sigma \{ (\sinh kz_i - \sinh kz_{i-1})$$
$$/ (k \sinh kh) \} \mid \cos \sigma t \mid . \quad \cdots\cdots\cdots\cdots (14)$$
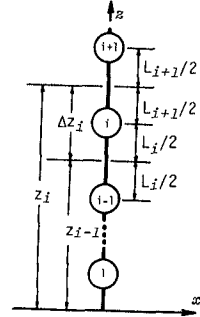
Fig.5 Range of the integration.

The wave forces acting on the mass i can be expressed as follows:

$$f_i(t) = X_i \cos \sigma t \mid \cos \sigma t \mid + Y_i \sin \sigma t , \quad \cdots\cdots\cdots\cdots\cdots\cdots (15)$$

in which,

$$X_i = C_D' (a^2 gk / \sinh 2kh) \{ (\sinh 2kz_i - \sinh 2kz_{i-1}) / 2k + \Delta z_i \} , \quad \cdots\cdots (16)$$

$$Y_i = -C_M' (ag / \cosh kh) (\sinh kz_i - \sinh kz_{i-1}) . \quad \cdots\cdots\cdots\cdots\cdots\cdots (17)$$

If we expand the part $\cos \sigma t \mid \cos \sigma t \mid$ in Eq.(15) into the Fourier series and take up to the third term, the Eq.(15) yields

$$f_i(t) = \frac{8}{3\pi} X_i \cos \sigma t + \frac{8}{15\pi} X_i \cos 3\sigma t - \frac{8}{105\pi} X_i \cos 5\sigma t + Y_i \sin \sigma t . \quad \cdots\cdots\cdots\cdots (18)$$

It can be recognized that the four terms $(8/3\pi)X_i$, $(8/15\pi)X_i$, $(8/105\pi)X_i$ and Y_i are generated as the amplitudes of external forces f_{z_i} included in $[P]_i$ of Eq.(5), and that Ω_i in this case becomes Ω, 3Ω, 5Ω and Ω corresponding to each amplitude. Therefore, in order to obtain the actual state vector including the time part, each $\{z\}$ must be calculated by using each f_{z_i} and Ω_i. Then each $\{z\}exp(j\Omega t)$ must be calculated, and the real part or imaginary part of $\{z\}exp(j\Omega t)$ must be chosen whether the phase of the terms of external force is cos or sin respectively. Finally, these must be composed.

In the actual calculations, f_ψ, $I_y \Omega^2$ and $c_\psi \Omega$ included in Eq.(5) are all neglected because they are ascertained as not greatly effecting the values of state vectors by performing some model calculations. Moreover, c_1 in c_{z_i} of Eq.(14) is also neglected because of being small compared with $2C_D' \mid u \mid$.

RESONANCE OF PILE DUE TO SMALL AMPLITUDE WAVE

     In order to explain some characteristics of the vibrations of a
vertical circular cylinder, some calculations have been performed by
using the method indicated above. The calculating conditions are
determined by considering the scale of the experiments.
     The water depth h is 40cm. The diameter of the cylinder D is 3cm,
the length 60cm, the specific density 1.12, and the elastic modulus E
500Kg/cm². It is inappropriate to always give the drag and inertia
coefficients C_D and C_M definite values, therefore they should be changed
according to the various cases. Practically, however, it is difficult to
choose appropriate values in each case because these values cannot be
determined only by the Reynolds number and Keulegan-Carpenters' number[5]
In this paper, therefore, C_M=2.0 and C_D=1.0 were ventured to be used as
the design criteria[6]in all cases. Moreover, the added mass coefficient K
is fixed to 1.0 and structural damping is neglected as ε=0. The cylinder
is idealized by 6 masses and 7 beams as shown in Fig.3. The lengths of
the beams are 5cm at the locations of the fixed bottom and top, and 10cm
at the other locations.
     Fig.6 shows the characteristics of resonance, taking the horizontal
axis as wave period T and the vertical axis as maximum values of the
displacement at the top point in the direction of wave propagation. The
dotted lines in this figure indicate that the waves exceed their
breaking limit H/L=0.14.
     It can be seen from this figure that the resonance occurs at
T=0.44sec and 1.32sec (=3×0.44sec) because of the first and fourth terms
having the angular frequency σ , and the second term having 3σ in the
right hand side of Eq.(18), respectively. However, as the wave height
increases, the resonant effects at T=2.20sec (=5×0.44sec) become more
indistinguishable at the displacement of the positive side (not of the
negative side) because of the negative sign of the third term having the
angular frequency 5σ of Eq.(18).
     Generally speaking, the resonance of pile structures appears at the
wave periods of odd number intervals' natural period in the case where
the small amplitude wave theory is used.
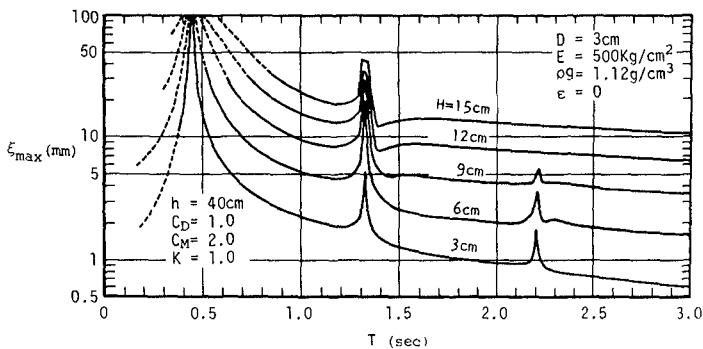
Fig.6 Characteristics of resonance due to small amplitude waves[4].

Fig.7 shows the time variations of the displacement at the top point during a cycle of waves by successively changing the wave periods. t/T=0 and ±0.5 express the phases of the wave crests and troughs coming to the position of the cylinder respectively. The displacements are divided by their maximum value in each case to standardize them. In all cases, the ratio of the maximum inertia forces to the maximum drag forces are 2:1. and therefore, the high frequency components of the drag forces are not so large. However, it can be seen from this figure that high frequency vibrations appear in the time variations of displacement in the cases T=1.30sec or 1.35sec and 2.20sec because of resonant effects.

RESONANCE OF PILE DUE TO STOKES WAVE

An experiment concerning vibrations of a circular cylinder has been performed at the Department of Civil Engineering of Kanazawa University. The experimental apparatus is shown in Fig.8. The dimension of the wave tank used in this experiment was 50cm wide, 60cm high and 14m long. A wave generator of the plunging type was installed at the end of this wave tank. A circular cylinder of which end the plate spring was attached was vertically installed 4.5m apart from this wave generator. The diameter of this cylinder D was 3cm, the length 60cm, the specific gravity 1.60, and the elastic modulus of the plate spring E 400Kg/cm^2. The dynamic displacements of this cylinder were measured at its top part, at which a copper plate was attached, by using the electromagnetic displacement meter of the non-contact type. The water depth h was 40cm.
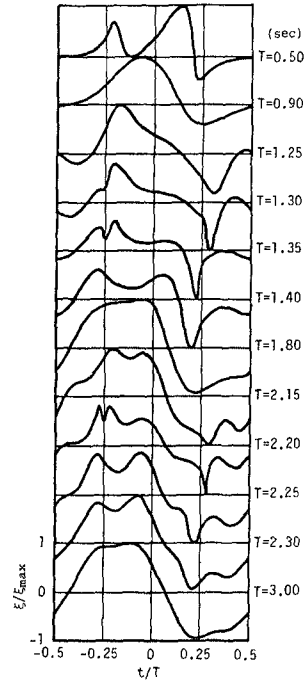

Fig.7 Time variations of the displacement at the top point of cylinder[4].
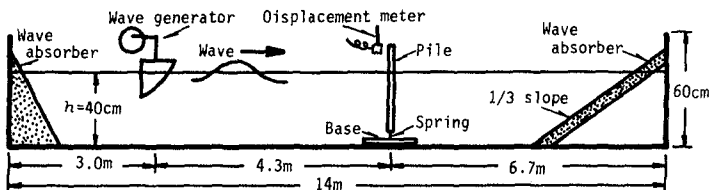
Fig.8 Experimental apparatus in the case of a pile.

     In this experiment, the resonance appeares by the waves of which
period is integer times natural period of the cylinder. This phenominum
cannot be explained by using the small amplitude wave theory but the
Stokes wave theory. This reason is that the inertia force contains the
frequency terms of $sin\sigma t$, $sin2\sigma t$, $sin3\sigma t$, $sin4\sigma t$,... and the drag force
produces the frequency terms $cos\sigma t$, $cos2\sigma t$, $cos3\sigma t$, $cos4\sigma t$,... when the
Stokes wave theory is applied to the Morison's formula.
     Fig.9 shows the comparrison between the experimental data and the
calculated values by using the small amplitude wave theory and the
Stokes wave theory. In this figure, it is recognized that the calculated
values by using the Stokes wave theory agree roughly well with the
experimental ones near the resonant point $T=0.71$sec which is two times
the natural period of cylinder $T=0.354$sec.

Fig.9

Characteristics
of resonance in
the   case   of
small   diameter
cylinder due to
Stokes wave.
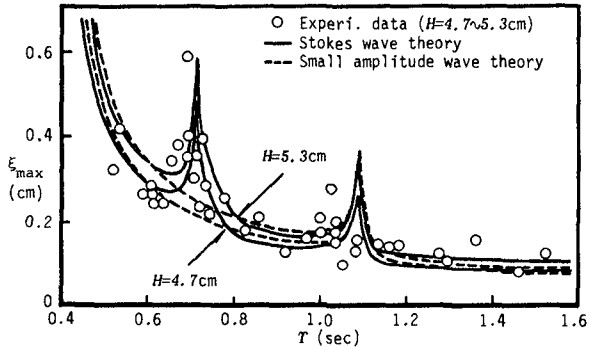
DYNAMIC RESPONSE OF PLATFORM

     In the case of a platform, the axial force N and its displacement u
shown in Fig.10 should be introduced. Therefore, the state vector is
denoted as follows:

$$\{z\}=\{u,-w,\psi,M_y,V_z,N\,|\,u,-w,\psi,M_y,V_z,N\,|\,1\}^T\cdots\cdots(19)$$

              Real   Imaginary Unit

     The   portion   of   the   corner   idealized   as
mass-beam system is shown in Fig.11, in which the
corner transfer matrix [C] is newly introduced to
change the direction of the nutral axis at the
corner. The corner transfer matrix is indicated by
Eq.(20) in the case that the nutral axis turns 270
degrees clockwise. The point transfer matrix and the
field transfer matrix are indicated by Eqs.(21) and
(22)   respectively.   The   state   vectores   can   be
determined by multiplying these matices in the same
manner as the vertical pile[1].

Fig.10 Coordinate
       system.

Fig.11 Mass-beam system at the corner.

$$[C] = \left(\begin{array}{ccc|ccc|ccc|ccc|c}
0 & -1 & 0 & & & & & & & & & & 0 \\
1 & 0 & 0 & & 0 & & & 0 & & & 0 & & 0 \\
0 & 0 & 1 & & & & & & & & & & 0 \\ \hline
 & & & 1 & 0 & 0 & & & & & & & 0 \\
 & 0 & & 0 & 0 & -1 & & 0 & & & 0 & & 0 \\
 & & & 0 & 1 & 0 & & & & & & & 0 \\ \hline
 & & & & & & 0 & -1 & 0 & & & & 0 \\
 & 0 & & & 0 & & 1 & 0 & 0 & & 0 & & 0 \\
 & & & & & & 0 & 0 & 1 & & & & 0 \\ \hline
 & & & & & & & & & 1 & 0 & 0 & 0 \\
 & 0 & & & 0 & & & 0 & & 0 & 0 & -1 & 0 \\
 & & & & & & & & & 0 & 1 & 0 & 0 \\ \hline
0 & 0 & 0 & 0 & 0 & 0 & 0 & 0 & 0 & 0 & 0 & 0 & 1
\end{array}\right).$$ ···(20)

$$[P]_i = \left(\begin{array}{cccccc|cccccc|c}
1 & 0 & 0 & 0 & 0 & 0 & 0 & 0 & 0 & 0 & 0 & 0 & 0 \\
0 & 1 & 0 & 0 & 0 & 0 & 0 & 0 & 0 & 0 & 0 & 0 & 0 \\
0 & 0 & 1 & 0 & 0 & 0 & 0 & 0 & 0 & 0 & 0 & 0 & 0 \\
0 & 0 & 0 & I_y\Omega^2 & 1 & 0 & 0 & 0 & c_\phi\Omega & 0 & 0 & 0 & -f_\psi \\
0 & m\Omega^2 & 0 & 0 & 1 & 0 & 0 & c_z\Omega & 0 & 0 & 0 & 0 & -f_x \\
-m\Omega^2 & 0 & 0 & 0 & 0 & 1 & -c_x\Omega & 0 & 0 & 0 & 0 & 0 & -f_x \\ \hline
0 & 0 & 0 & 0 & 0 & 0 & 1 & 0 & 0 & 0 & 0 & 0 & 0 \\
0 & 0 & 0 & 0 & 0 & 0 & 0 & 1 & 0 & 0 & 0 & 0 & 0 \\
0 & 0 & 0 & 0 & 0 & 0 & 0 & 0 & 1 & 0 & 0 & 0 & 0 \\
0 & 0 & -c_\phi\Omega & 0 & 0 & 0 & 0 & 0 & I_y\Omega^2 & 1 & 0 & 0 & 0 \\
0 & -c_z\Omega & 0 & 0 & 0 & 0 & 0 & m\Omega^2 & 0 & 0 & 1 & 0 & 0 \\
c_x\Omega & 0 & 0 & 0 & 0 & 0 & -m\Omega^2 & 0 & 0 & 0 & 0 & 1 & 0 \\ \hline
0 & 0 & 0 & 0 & 0 & 0 & 0 & 0 & 0 & 0 & 0 & 0 & 1
\end{array}\right)_i.$$ ···(21)

$$[F]_i = \left(\begin{array}{cccccc|cccccc|c}
1 & 0 & 0 & 0 & 0 & \dfrac{L}{EA(1+\varepsilon^2)} & 0 & 0 & 0 & 0 & 0 & \dfrac{\varepsilon L}{EA(1+\varepsilon^2)} & 0 \\
0 & 1 & L & \dfrac{L^2}{2EI(1+\varepsilon^2)} & \dfrac{L^3}{6EI(1+\varepsilon^2)} & 0 & 0 & 0 & 0 & \dfrac{\varepsilon L^2}{2EI(1+\varepsilon^2)} & \dfrac{\varepsilon L^3}{6EI(1+\varepsilon^2)} & 0 & 0 \\
0 & 0 & 1 & \dfrac{L}{EI(1+\varepsilon^2)} & \dfrac{L^2}{2EI(1+\varepsilon^2)} & 0 & 0 & 0 & 0 & \dfrac{\varepsilon L}{EI(1+\varepsilon^2)} & \dfrac{\varepsilon L^2}{2EI(1+\varepsilon^2)} & 0 & 0 \\
0 & 0 & 0 & 1 & L & 0 & 0 & 0 & 0 & 0 & 0 & 0 & 0 \\
0 & 0 & 0 & 0 & 1 & 0 & 0 & 0 & 0 & 0 & 0 & 0 & 0 \\
0 & 0 & 0 & 0 & 0 & 1 & 0 & 0 & 0 & 0 & 0 & 0 & 0 \\ \hline
0 & 0 & 0 & 0 & 0 & \dfrac{-\varepsilon L}{EA(1+\varepsilon^2)} & 1 & 0 & 0 & 0 & 0 & \dfrac{L}{EA(1+\varepsilon^2)} & 0 \\
0 & 0 & 0 & \dfrac{-\varepsilon L^2}{2EI(1+\varepsilon^2)} & \dfrac{-\varepsilon L^3}{6EI(1+\varepsilon^2)} & 0 & 0 & 1 & L & \dfrac{L^2}{2EI(1+\varepsilon^2)} & \dfrac{L^3}{6EI(1+\varepsilon^2)} & 0 & 0 \\
0 & 0 & 0 & \dfrac{-\varepsilon L}{EI(1+\varepsilon)^2} & \dfrac{-\varepsilon L^2}{2EI(1+\varepsilon^2)} & 0 & 0 & 0 & 1 & \dfrac{L}{EI(1+\varepsilon^2)} & \dfrac{L^2}{2EI(1+\varepsilon^2)} & 0 & 0 \\
0 & 0 & 0 & 0 & 0 & 0 & 0 & 0 & 0 & 1 & L & 0 & 0 \\
0 & 0 & 0 & 0 & 0 & 0 & 0 & 0 & 0 & 0 & 1 & 0 & 0 \\
0 & 0 & 0 & 0 & 0 & 0 & 0 & 0 & 0 & 0 & 0 & 1 & 0 \\ \hline
0 & 0 & 0 & 0 & 0 & 0 & 0 & 0 & 0 & 0 & 0 & 0 & 1
\end{array}\right)_i.$$ ···(22)

The experiment has been carried out to the platform shown in Photo. 1 . Four vertical piles supporting the aluminum plate are made of rubber, and their diameter is 3cm, the elastic modulus 600Kg/cm². Idealizing this platform as mass-beam system as shown in Fig.12, the analyses have been performed by using the small amplitude wave theory to simplify the calculations.

One of the model calculations about resonance is shown in Fig.13, in which the horizontal axis is the wave period T, and the vertical one is the maximum value of the displacement at the corner point B. The wave steepness is kept $H/L = 0.1$, and the added mass coefficient K is changed 0, 1 and 2. From this figure, it can be seen that the resonant wave period decreases as K decreases from 2 to 0, and the value of the displacement becomes minimum at the wave period $T = 0.54$sec. The minimum point of the displacement appears when the wave length becomes about two times distance between piles because the directions of wave forces acting on the piles become opposite with each other.
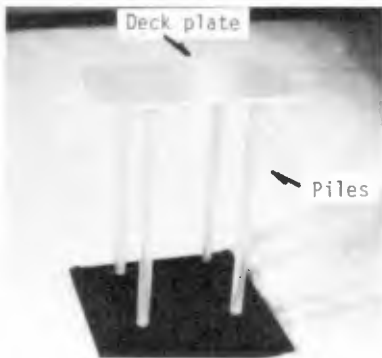
Photo.1 Model of platform.
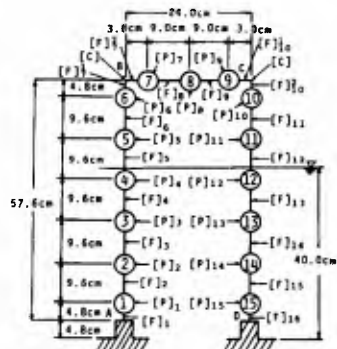
Fig.12 Idealized platform
as mass-beam system.
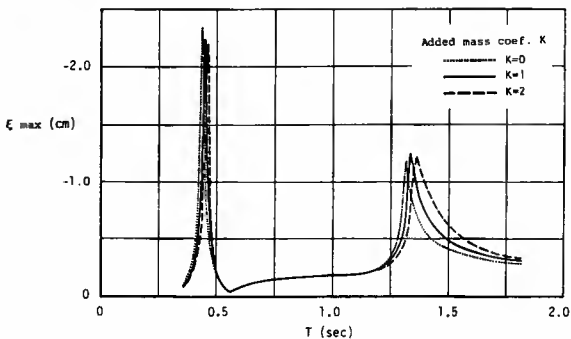
Fig.13 Characteristics of resonance of the platform.

Fig.14 shows the comparison of the time variations of the displacement at the point B between the experimental values and the calculated ones. From this figure, it is recognized that the calculated values shown by chain lines agree well with the experimental ones shown by solid lines.
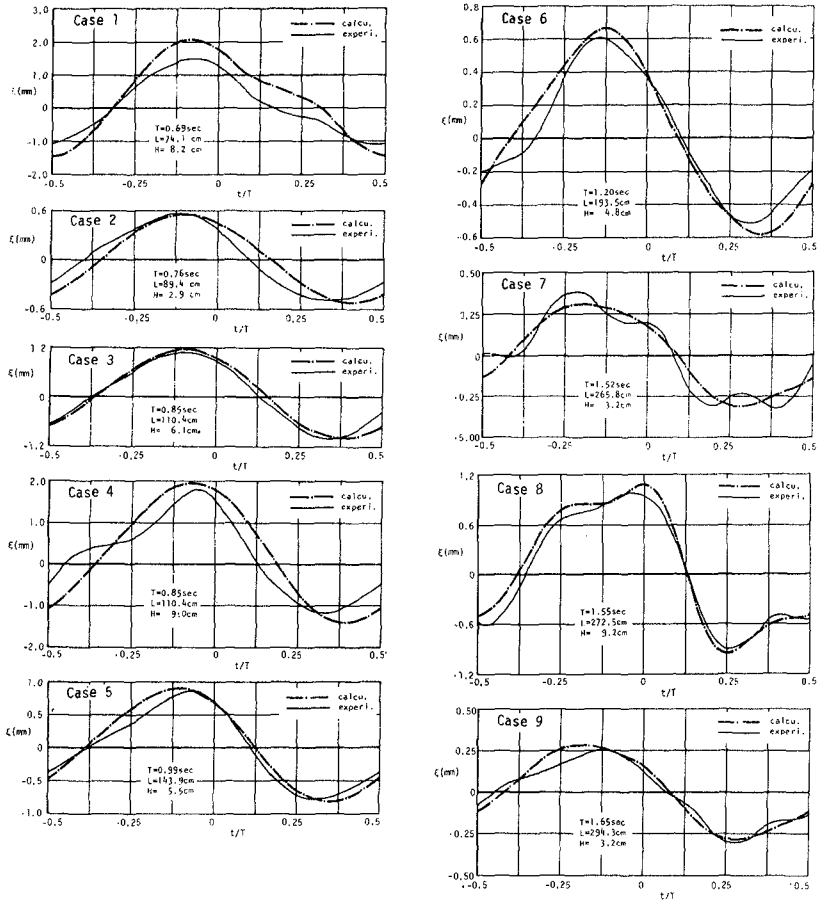
Fig.14   Comparison of the time variations of displacement
         between the experimental values and the calculated.

DYNAMIC RESPONSE OF LARGE DIAMETER PILE

In the case of a large diameter pile, MacCamy-Fuchs﹐ diffraction theory can be applied to the equation of wave forces instead of Morison's formula in its calculations. On the occasion of this experiment, the circular cylinder shown in Fig.15 has been used. The diameter of this cylinder is 40cm and the experimental apparatus is shown in Photo.2. The dimension of the wave tank is 6.7m long, 4.3m wide and 55cm deep. The water depth was kept 35cm, and the displacement was measured by using the contact type displacement meter. The natural period of this cylinder is 0.56sec in the still water.

Fig.16 shows the characteristic of resonance of this cylinder with comparing the experimental values with the calculated ones. From this figure it is recognized that the solid line calculated by using $K=0$ is closer to the experimental values than the broken line calculated by using $K=1$. This fact may indicates that the added mass coefficient K decreases from 1.0 with according to the increase in magnitude of the displacement.
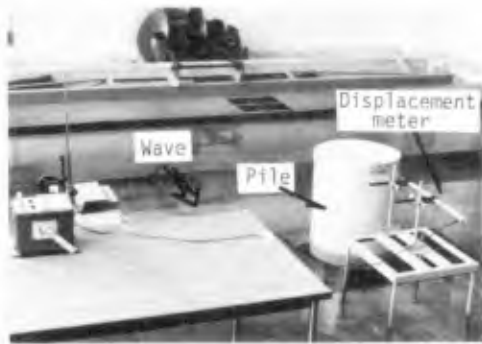
Photo.2 Experimental apparatus.
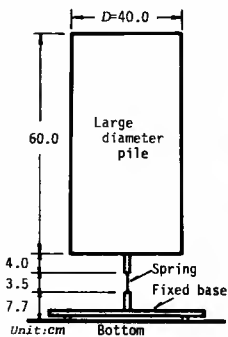
Fig.15 Large diameter pile.
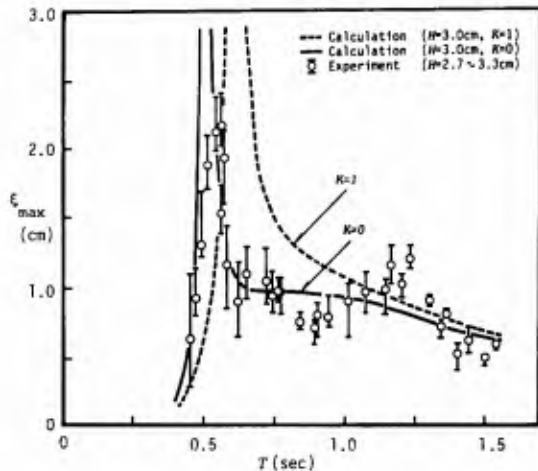
Fig.16 Caracteristics of resonance.

METHOD OF STRUCTURAL-PROPERTY MATRICES

EVALUATION OF STRUCTURAL-PROPERTY MATRICES

The method of transfer matrices has been proved most effective for the analysis of harmonic vibrations. On the other hand, the method of structural property matrices is available for the non-harmonic vibrations. In this approach, the structure is assumed to be divided into a system of discrete elements which are interconnected only at a finite number of nodal point. The properties of the complete structure are then found by evaluating the properties of the individual finite elements and superposing them appropriately[3].

Fig.17 shows the beam element of number i, in which the displacements and rotations at node i and i-1 are denoted by ξ_i, ξ_{i-1} and θ_i, θ_{i-1} respectively. The deflected shape of the element $\xi(x)$ can be expressed in terms of its nodal rotations and displacements as follows:

$$\xi(x) = \psi_1(x)\xi_{i-1} + \psi_2(x)\xi_i + \psi_3(x)\theta_{i-1} + \psi_4(x)\theta_i \, , \cdots (23)$$

in which, $\psi_n(x)$ (n=1,2,3,4) are the deflections developed in the element subjected to the unit nodal displacements which can be expressed as follows:

Fig.17 Notation of forces and displacements at beam element.

$$
\left.
\begin{aligned}
&\text{for } \xi_{i-1}=1; \quad \psi_1(x) = 1 - 3\,(x/l\,)^2 + 2\,(x/l\,)^3 \\
&\text{for } \xi_i \;\;=1; \quad \psi_2(x) = 3\,(x/l\,)^2 - 2\,(x/l\,)^3 \\
&\text{for } \theta_{i-1}=1; \quad \psi_3(x) = x\,(1 - x/l\,)^2 \\
&\text{for } \theta i \;\;=1; \quad \psi_4(x) = (x^2/l\,)\,(x/l - 1\,)
\end{aligned}
\right\} \cdots\cdots\cdots\cdots\cdots\cdots (24)
$$

Here, the displacement vector of i-th beam is defined in terms of its nodal rotations and displacements as follows:

$$u_i = (\,\xi_{i-1}, \;\theta_{i-1}, \;\xi_i, \;\theta_i\,)^{\mathrm{T}} . \cdots\cdots\cdots\cdots\cdots\cdots (25)$$

The external forces and moments applied to a beam element are assumed to act only upon its nodes as shown in Fig.17. The force vector of i-th beam is defined in terms of these forces and moments as follows:

$$F_i = (\,P_{i-1}^i, \;M_{i-1}^i, \;P_i^i, \;M_i^i\,)^{\mathrm{T}} . \cdots\cdots\cdots\cdots\cdots\cdots (26)$$

When the force vector F_i acts upon the i-th element, the equation of motion about the i-th element is given as follows:

$$[M]_i \; \ddot{u}_i + [C]_i \; \dot{u}_i + [K]_i \; u_i = F_i \; , \quad \cdots\cdots\cdots\cdots\cdots\cdots\cdots (27)$$

in which, $[K]_i$ $[M]_i$ and $[C]_i$ are called the stiffness matrix, the mass matrix and the damping matrix respectively. By applying the principle of virtual work to the element, these matrices can be evaluated as shown in Eqs.(28), (29) and (30) respectively, in which, $\psi_n'' = d^2\psi_n / dx^2$, $\bar{m}$ and $\bar{c}$ is the mass and the damping coefficient per unit length which can be calculated from Eqs.(13) and (14) respectively. Moreover, the force vectors can be evaluated by using the Morison's formula, and however, the moments may be neglected when their magnitudes are small.

Evaluating the equations of motion for the individual finite elements and superposing them, the equation of motion for the complete structure can be obtained. The time variations of the displacement vectors can be calculated from this equation.

$$[K]_i = \left[EI \int_0^l \psi_j'' \psi_k'' dx \right]_i = \left(\frac{2EI}{l^3} \right) \begin{bmatrix} 6 & 3l & -6 & 3l \\ & 2l^2 & -3l & l^2 \\ & & 6 & -3l \\ \text{Sym.} & & & 2l^2 \end{bmatrix}_i , \quad \cdots\cdots\cdots (28)$$

$$[M]_i = \left[\bar{m} \int_0^l \psi_j \psi_k dx \right]_i = (\bar{m} l)_i \begin{bmatrix} \frac{13}{35} & \frac{11}{210}l & \frac{9}{70} & -\frac{13}{420}l \\ & \frac{1}{105}l^2 & \frac{13}{420}l & -\frac{1}{140}l^2 \\ & & \frac{13}{35} & -\frac{11}{210}l \\ \text{Sym.} & & & \frac{1}{105}l^2 \end{bmatrix}_i , \quad \cdots\cdots\cdots (29)$$

$$[C]_i = \left[\bar{c} \int_0^l \psi_j \psi_k dx \right]_i = \left(\frac{\bar{c}}{\bar{m}} \right)_i [M]_i \quad \cdots\cdots\cdots\cdots\cdots\cdots\cdots\cdots (30)$$

TIME VARIATION OF PILE DISPLACEMENT

Some experiments and calculations have been performed for the small diameter cylinder, of which end the plate spring is attached. The length of this cylinder is 60cm and the diameter is 4cm. The flexural rigidity of the plate spring EI is 1.93×10^5 Kg.cm^2. The natural period of the cylinder was changed appropriately by arranging the length of plate spring. In the experiment, the water depth was always kept 40cm. In the calculations, this cylinder is divided into seven elements as shown in Fig.18. The Newmark's β method has been applied to calculate the time variations of the displacement vector with selecting $\beta=0.25$.
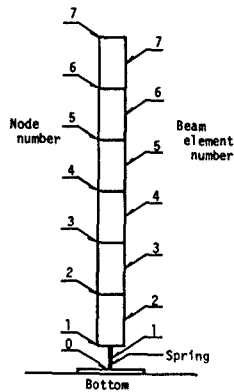

Fig.18 Division of pile into elements.

Fig.19 shows the time variations of the displacement at the
cylinder top, in which the dotted lines and solid lines indicate the
experimental values and the calculated ones respectively. In Fig.19(a),
the displacements become larger to a certain magnitude as the time
proceeds, because the wave period T=0.84sec is close to the natural
period 0.80sec. In Fig.19(b), the displacements are beating, because the
wave period T=0.92sec is slightly different from the natural period. In
Fig.19(c), the calculated values agree well with the experimental.
    Fig.20 is one of the examples applied to the case of hyperbolic
waves, in which the upper figure shows the water level variation η and
the lower one is the displacement ξ calculated from η. In the
displacement, the natural vibrations are generated by the high frequency
component waves included in the wave crests.
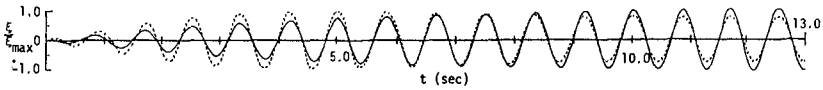
(a) T=0.84sec, H=1.9cm, ξ_{max}=4.85cm.
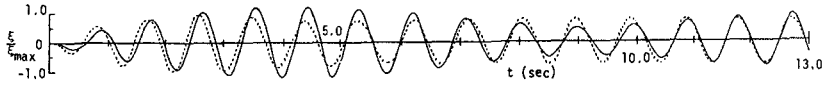
(b) T=0.92sec, H=4.1cm, ξ_{max}=4.91cm.
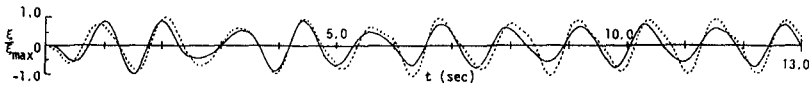
(c) T=1.18sec, H=4.6cm, ξ_{max}=1.98cm.

Fig.19   Time variations of displacement of small diameter pile.
          (Solid line: Calculated.   Dotted line: Experiment)
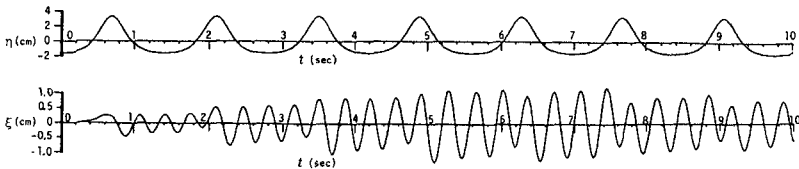
Fig.20   Time variations of hyperbolic waves and
          the displacement of small diameter pile.

In the case of irregular waves, ξ can be calculated only from η by using the linear filters[7]. Fig.21 is one of the examples of irregular waves, in which, the calculated values of the displacement shown by solid line agree well with the experimental ones shown by dotted line.
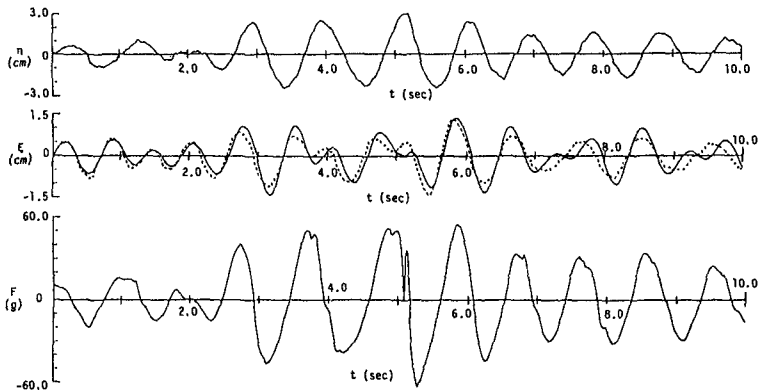
Fig.21 Time variations of displacements in case of irregular wave. (η: water level variation, ξ: displacement, F: wave force)

CONCLUSIONS

The harmonic vibrations of structures can be calculated by the method of transfer matrices. On the other hand, in order to calculate the transient response with considering initial conditions or the random vibrations induced by irregular waves, the method of structural-property matrices should be used. In these calculations, the added mass coefficient should be given an appropriate value in the range from 0 to 1 in accordance with the magnitude of a displacement, and also the damping coefficient should be determined with considering the interaction effect between structures and waves.

The resonance of a small diameter pile occures at the wave periods of integer times natural period, which has been confirmed by the experiments and the calculations. The time variations of the displacement of structures can be calculated correctly by using the matrix methods shown in this paper.

ACKNOWLEDGEMENT

REFERENCES

1) Gaither,W.S. and D.P.Billington "The dynamic response of offshore structures to time dependent forces", Proc. 9th Conf. on Coastal Engg., pp.453-471, 1964.

2) Sarpkaya,T. and M.Isaacson "Mechanics of wave forces on offshore structures", Van Nostrand Reinhold Company, pp.381-472, 1981.

3) Clough,R.W. and J.Penzien "Dynamics of structures", MacGraw-Hill, 1975.

4) Hajime Ishida "Dynamic response of vertical pile to periodic waves by transfer matrix method", Symposium Engg. in Marine Environment, in Brugge, pp.2.102-2.114, 1982.

5) Iwagaki,Y., Ishida,H. and T.Senda "Irregular wave forces on a circular cylinder", Proc. 20th Conf. on Coastal Engg. in Japan, pp.1-5, 1973. (in Japanese)

6) JSCE "Index to design offshore steel structures", JSCE, 1973. (in Japanese)

7) Ishida,H. and Y.Iwagaki "Wave forces induced by irregular waves on a vertical circular cylinder", Proc. 16th Conf. on Coastsl Engg., pp.2397-2414, 1979.